

Integrating Sub-6 GHz and Millimeter Wave to Combat Blockage: Delay-Optimal Scheduling

Guidan Yao*, Morteza Hashemi†, and Ness B. Shroff *‡

* Department of Electrical and Computer Engineering, Ohio State University

†Department of Electrical Engineering and Computer Science, University of Kansas (KU)

‡Department of Computer Science and Engineering, Ohio State University

Abstract—Millimeter wave (mmWave) technologies have the potential to achieve very high data rates, but suffer from intermittent connectivity. In this paper, we provision an architecture to integrate sub-6 GHz and mmWave technologies, where we incorporate the sub-6 GHz interface as a fallback data transfer mechanism to combat blockage and intermittent connectivity of the mmWave communications. To this end, we investigate the problem of scheduling data packets across the mmWave and sub-6 GHz interfaces such that the average delay of system is minimized. This problem can be formulated as Markov Decision Process. We first investigate the problem of discounted delay minimization, and prove that the optimal policy is of the threshold-type, i.e., *data packets should always be routed to the mmWave interface as long as the number of packets in the system is smaller than a threshold*. Then, we show that the results of the discounted delay problem hold for the average delay problem as well. Through numerical results, we demonstrate that under heavy traffic, integrating sub-6 GHz with mmWave can reduce the average delay by up to 70%. Further, our scheduling policy substantially reduces the delay over the celebrated MaxWeight policy.

I. INTRODUCTION

The annual amount of mobile data is projected to surpass 130 exabits by 2020 [1]. With such rapid increases in mobile data traffic, we are facing unprecedented challenges due to the shortage of wireless spectrum. To mitigate the problem of spectrum scarcity, the millimeter wave (mmWave) band, ranging from 30 GHz to 300 GHz, provides a promising solution [2]. However, before mmWave communications can become a reality, there exist several significant challenges that need to be overcome. In particular, mmWave channels can be highly variable with intermittent on-off periods. Due to small wavelengths in the mmWave band, most objects, such as concrete walls, a human body or even rain drops, may cause blocking and reflections as opposed to scattering and diffraction in the sub-6 GHz frequencies. In this case, blockage may completely break the mmWave link and result in an almost zero delivery rate [3, 4]. In the provisioned applications of mmWave, human blockage is one of the main challenges that can increase the path loss by more than 20 dB [5, 6].

To demonstrate the effect of human blockage on mmWave links, we have conducted a set of measurements with a stationary transmitter and a mobile receiver that moves away from the transmitter with the speed of 1 m/s. During the time intervals 200–300 and 500–600 ms, a human body blocks the line-of-sight (LOS) path between the transmitter and receiver.

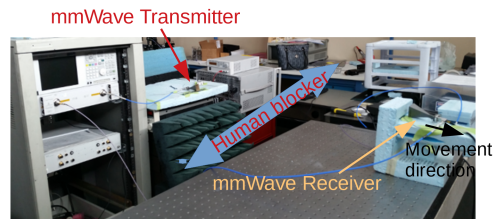


Fig. 1: Measurement setup and experiment scenario to investigate the effect of human blockage on mmWave channels.

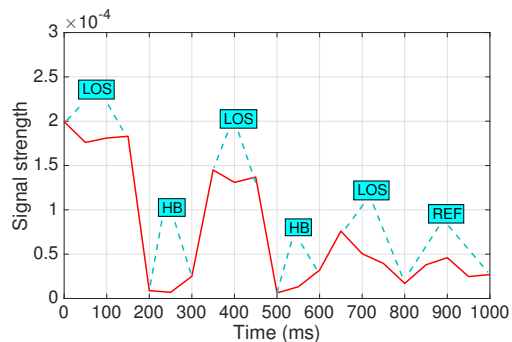


Fig. 2: Received mmWave signal strength under line of sight (LOS), human blocker (HB), and reflection (REF) [7].

Figure 1 shows our basic experimental setup, and Fig. 2 depicts the strength of received signal at the mobile receiver over time [7]. From the results, we see that the received signal strength falls to almost zero under blockage, which can be modeled as an OFF or unavailable period. Therefore, the mmWave link exhibits an ON/OFF connectivity pattern under blockage scenarios such that during the OFF periods, delivery rate and delay performance can highly degrade.

In order to mitigate the effects of intermittent connectivity, especially for delay-sensitive applications, several methods have been proposed. For instance, the authors in [4] and [8] exploit reflection paths and multi-hop paths to combat blockage. These methods are *reactive* in the sense that the search for an alternative path is triggered after blockage occurs. However, since the link speed of the mmWave interface (multi-Gbps) is comparable to the speed at which a typical processor in a smart device operates, these methods may not be able to track and respond to channel variations in real-time. Therefore, it necessitates the use of a reasonably large

buffer at the mmWave interface along with *proactive solutions* to complement this design. In addition to the aforementioned methods, there exist several works on integrating the mmWave and sub-6 GHz technologies. For instance, information of the sub-6 GHz channel is extracted to reduce mmWave beam-forming overhead [9, 10], while [11] uses an online learning method. The authors in [7, 12, ?] consider resource allocation and cooperative communication between the sub-6 GHz and mmWave to maximize either the throughput of the system or the quality-of-service per user application.

Although an integrated mmWave/sub-6 GHz architecture has been previously proposed, the delay minimization problem in this integrated architecture has not been explored yet. In this paper, we exploit the sub-6 GHz interface as a fallback data transfer mechanism such that packets may be routed to the sub-6 GHz interface upon arriving at the system. Moreover, packets are allowed to be impatient in the sense that they *renege* from the mmWave interface to the sub-6 GHz interface, when the waiting time of the head-of-line packet in the mmWave interface becomes large. Within this content, we investigate the problem of delay-optimal scheduling across the sub-6 GHz and mmWave interfaces and obtain a proactive scheduling policy that is expressed in terms of the queue length of each component that constitutes the system.

The most relevant research to our delay minimization problem is the *slow-server* problem, in which the goal is to obtain a delay optimal scheduling policy in a queuing system with heterogeneous (i.e., fast and slow) servers. The goal of this problem is to investigate the trade-off between waiting in queue and entering slow servers when fast servers are busy. The slow-server problem was first proposed in [13], where the authors presented a M/M/2 queuing system with two heterogeneous servers and conjectured that the optimal policy for minimizing the average delay and expected total discounted delay in system is of the threshold-type. The conjecture was then proved in [14] with policy iteration. Later, papers [15] and [16] showed the same result with coupling arguments and value iteration, respectively. Following these works, [17] extended the result to the system with multi-servers (i.e., more than two), and [18, 19] studied the delay minimization problem with different arrival and service processes. In this context, the mmWave interface acts as the fast server with the presence of unavailable service under blockage.

Our delay minimization problem differs from the previous works in two key aspects: 1) Tandem queues exist in one branch of two parallel queues (see Fig. 4). This implies that our architecture is a mix of tandem and parallel queues, which is different from the parallel structure in slow-server problem; 2) Introduction of renegeing action complicates relationships among actions, i.e. we have to further consider the trade-off between waiting in the mmWave interface and renegeing to the sub-6 GHz as well (details are discussed in section II). In summary, our main contributions are as follows:

- We investigate the policy that minimizes the *expected total discounted delay* and through value iteration of Markov Decision Process (MDP), we obtain three rules

that partially characterize the optimal policy. Based on the findings, we propose a threshold-type policy with regard to the sub-6 GHz interface. Then, we collapse our system state space from four dimension to three dimension, and further demonstrate the optimality of the proposed policy. We further show that the proposed policy is also optimal for the *average delay problem*.

- We provide a methodology for solving the delay minimization problem in settings consisting of tandem and parallel queues with heterogeneous servers.
- Through simulations, we show that it is important to use the sub-6 GHz interface especially when the mmWave is unavailable with high probability and confirm that such a threshold-type policy improves the average delay performance while achieving similar throughput performance as the throughput-optimal and well-studied MaxWeight policy [20].

We use the following notations throughout the paper. Non-bold lowercase and uppercase letters are used for scalars and sets, respectively. Bold lowercase letters are used for vectors, $\mathbb{E}[\cdot]$ denotes the expectation operator, and the sub-6 GHz and mmWave variables are denoted by $(\cdot)_{\text{sub-6}}$ and $(\cdot)_{\text{mm}}$, respectively.

II. PROBLEM SETUP

In this section, we present the system model and formulate the delay minimization problem.

A. System Model

We consider an integrated communication architecture with dual sub-6 GHz and mmWave interfaces as shown in Fig. 3. The infinite *head buffer* is utilized to store all packets waiting to be processed and served by either mmWave or sub-6 GHz. The *processing server* is responsible for essential data processing before scheduling. Plus, the system includes two servers (mmWave and sub-6 GHz servers) with extremely different service rates, i.e. the service rate of mmWave can be 100 times larger than the service rate of sub-6 GHz.

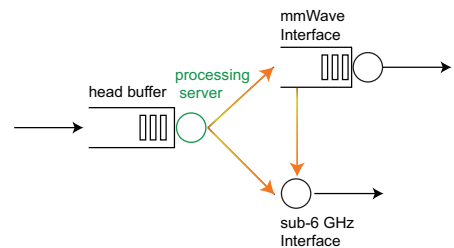


Fig. 3: Integrated sub-6 GHz and mmWave architecture.

(i) Queue Models: In our system model, we add a buffer to the mmWave interface, which stores packets routed from the head buffer. The rationality of our design (i.e., a separate queue for the mmWave interface) is described next. The service rate of the mmWave server is comparable to the processing server (i.e., processor speed). Moreover, mmWave is very sensitive to blockage which is hard to predict. If we assume that there is no buffer for the mmWave server, then every packet has to wait in

the head queue until the mmWave server is empty. In the case, the packet will experience service time of both the processing and the mmWave servers (almost double the service time of the mmWave) except waiting time in the head buffer. Then, the performance of mmWave is degraded by approximately half. On the contrary, if the mmWave server has its own buffer for processed packets, part of waiting time in the head buffer can be utilized to process packets in advance, which reduces the experienced service time mentioned above. However, the sub-6 GHz link is much slower than the processing server. Therefore, processing delay can be ignored compared to service time of the sub-6 GHz. In other words, it is not necessary for the sub-6 GHz server to have its own buffer considering the cost of buffer. Thus, it is appropriate to assume that the *sub-6 GHz interface* acts as a server with a buffer size of one, while the *mmWave interface* consists of an infinite buffer and a server. Since delay of the processing server becomes negligible compared with the sub-6 GHz interface, we consider the equivalent model depicted in Fig. 4, where we call the processing server and mmWave interface as *mmWave line*.

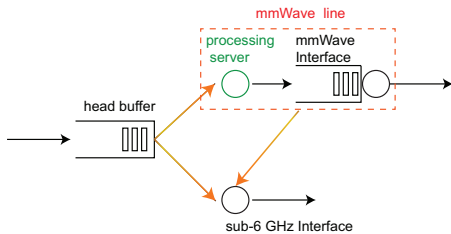


Fig. 4: Equivalent system model.

(ii) Two-state mmWave link; Available or Unavailable:

Recall that the mmWave link is highly variable with intermittent ON/OFF periods. It is reasonable to model the mmWave service rate with two states, say *available* and *unavailable*. For the unavailable state, the mmWave channel is almost disconnected and thus we assume that the service rate of the mmWave is 0. For the available state, we assume that the service time is exponentially distributed with parameter μ_{mm} . Further, we denote the probability of available and unavailable states with p_a and p_{na} , respectively.

We further assume that arrivals to the system form a Poisson process with parameter λ , and that service times of the processing server and the sub-6 GHz interface are exponentially distributed with parameter μ_p and $\mu_{\text{sub-6}}$, respectively. Given that the mmWave service rate is of the same order as the clock speed of the processor (i.e., several GHz), we assume that μ_p is much faster than $\mu_{\text{sub-6}}$ but in the same order as μ_{mm} .

Within this content, we further clarify the difference of our problem from previous work, which has been briefly discussed in section I. In Fig. 4, the mmWave line is a tandem queue system, which is parallel to the sub-6 GHz interface. In the case, to finally obtain the optimality of the proposed threshold-type policy, we need to show and utilize the relationship between the resulting delays starting at states with the packet in processing server and the packet moved to the mmWave queue, where the two states cannot be collapsed. This implies

that our problem is more complex than the classic slow-server problem.

Recall that to avoid a large waiting time in the mmWave queue due to intermittent channel, we require the packets to be *impatient* in the sense that if the waiting time of the head-of-line packet in the mmWave queue becomes large, the packet “reneges” (is moved to) from the mmWave line to the sub-6 GHz server. Note that the packet in the sub-6 GHz server cannot be sent back to the mmWave line or the head buffer. In the case, *when shall we use the slow server (the sub-6 GHz server)? Where shall we move packets from to sub-6 GHz, the mmWave line or the head buffer?* That is, despite trade-off between waiting in the head queue and entering the slow server which is investigated in the slow-server problem, our problem cares about the trade-off between waiting in the mmWave line and entering the slow server and trade-off between dispatching packets from the head buffer and the mmWave line.

B. System Dynamics

(i) System States: Let $q_0, q_1 \in \mathbb{N}$ denote the queue length of the head buffer and mmWave interface, respectively. Moreover, let l_1, l_2 denote busy/idle condition of the processing server and sub-6 GHz interface, respectively. Then, l_1, l_2 take values in $\{0, 1\}$, where $l_1 = 1$ implies a busy server. Therefore, the system state is expressed by a four-dimensional vector $\mathbf{q} \triangleq (q_0, l_1, q_1, l_2)$ with the state space $Q \triangleq \mathbb{N} \times \{0, 1\} \times \mathbb{N} \times \{0, 1\}$.

(ii) Events: There are four different events that happen in the system, which are defined as follows:

(1) *Arrival of a packet to the head buffer:*

$$A_0(\mathbf{q}) \triangleq (q_0 + 1, l_1, q_1, l_2).$$

(2) *Departure of a packet from the mmWave interface:*

$$D_1(\mathbf{q}) \triangleq (q_0, l_1, (q_1 - 1)^+, l_2),$$

where $(\cdot)^+ = \max(\cdot, 0)$.

(3) *Departure of a packet from the sub-6 GHz interface:*

$$D_2(\mathbf{q}) \triangleq (q_0, l_1, q_1, (l_2 - 1)^+).$$

(4) *Processing completion:* If the processing server delivers a packet to the mmWave interface, the system state changes as

$$\mathcal{T}(\mathbf{q}) \triangleq (q_0, (l_1 - 1)^+, l_1 + q_1, l_2).$$

Note that we introduce “dummy” packets for the last three events when $q_1 = 0, l_2 = 0$ and $l_1 = 0$, respectively. This is further elaborated in Section II-C.

(iii) Actions: $K = \{A_h, A_1, A_2, A_b, A_r\}$ is an action set. $K_{\mathbf{q}} \subseteq K$ denotes the set of admissible actions in state \mathbf{q} . Each action in set K is defined as follows:

(1) *Holding:* Action A_h keeps the system state unchanged, and is defined on Q . Therefore, we have

$$A_h(\mathbf{q}) \triangleq (q_0, l_1, q_1, l_2).$$

(2) *Scheduling-on-mmWave:* A packet can be routed to the mmWave line if the processing server is idle, i.e.,

$$A_1(\mathbf{q}) \triangleq (q_0 - 1, 1, q_1, l_2),$$

which is defined on the set $\{\mathbf{q} \mid q_0 \geq 1, l_1 = 0\}$.

(3) *Scheduling-on-sub-6*: A packet can be routed to the sub-6 GHz interface if the sub-6 GHz server is idle, i.e.,

$$A_2(\mathbf{q}) \triangleq (q_0 - 1, l_1, q_1, 1),$$

which is defined on the set $\{\mathbf{q} \mid q_0 \geq 1, l_2 = 0\}$.

(4) *Scheduling-on-both*: Action A_b dispatches two packets to the sub-6 GHz and processing servers simultaneously, i.e.,

$$A_b(\mathbf{q}) \triangleq (q_0 - 2, 1, q_1, 1),$$

which is defined on the set $\{\mathbf{q} \mid q_0 \geq 2, l_1 = l_2 = 0\}$.

(5) *Reneging*: Action A_r moves a packet from the mmWave line to the sub-6 GHz interface, and it is defined on the set $\{\mathbf{q} \mid q_1 + l_1 \geq 1, l_2 = 0\}$. Let A_{r_p} and $A_{r_{mm}}$ denote the renegeing actions from the processing server and mmWave interface, respectively. Therefore, we have

$$\begin{aligned} A_{r_p}(\mathbf{q}) &\triangleq (q_0, 0, q_1, 1), & \mathbf{q} \in \{\mathbf{q} \mid l_1 = 1, l_2 = 0\}; \\ A_{r_{mm}}(\mathbf{q}) &\triangleq (q_0, l_1, q_1 - 1, 1), & \mathbf{q} \in \{\mathbf{q} \mid q_1 \geq 1, l_2 = 0\}. \end{aligned}$$

Then, the renegeing action A_r is expressed as

$$A_r(\mathbf{q}) \triangleq \begin{cases} A_{r_p}(\mathbf{q}) & \text{if } l_1 = 1, q_1 = 0 \\ A_{r_{mm}}(\mathbf{q}) & \text{if } l_1 = 0, q_1 \geq 1 \\ \arg \min_{A_a \in \{A_{r_p}, A_{r_{mm}}\}} v(A_a(\mathbf{q})) & \text{otherwise} \end{cases}$$

where $v(\cdot)$ denotes the delay cost. Note that if A_{r_p} and $A_{r_{mm}}$ are admissible, we select an action that results in a smaller cost. In Section III, we show that $A_r = A_{r_p}$ for the discounted delay problem when both A_{r_p} and $A_{r_{mm}}$ are admissible.

C. Problem Formulation

Average Delay Problem: Our objective is to schedule packets across the mmWave and sub-6 GHz interfaces such that the average delay of system is minimized. To this end, we know that, by Little's Law, the average delay minimization problem is equivalent to minimizing the average total number of packets in the system, which is expressed as follows:

$$\min_{\pi \in \Pi} \limsup_{T \rightarrow \infty} \frac{1}{T} \mathbb{E}^\pi \left[\int_{t=1}^T (\mathbf{q}[t] \cdot \mathbf{e}) dt \right], \quad (1)$$

where \mathbb{E}^π denotes the conditional expectation given policy π , $\mathbf{q}[t] \in Q$ is the system state at time t , Π denotes the set of all admissible policies, and $\mathbf{e} = (1, 1, 1, 1)^T$. We model the system evolution as an MDP, and for simplicity, we convert the continuous-time MDP problem into an equivalent discrete-time MDP problem with the method of uniformization [21]. In particular, we assume that all servers will serve "dummy" packets whenever they are idle. Then, we separate continuous time into time slots with sequences when either a packet arrival or a packet (real or dummy) departure from the processing server or interfaces happens. Let $N = \{1, 2, 3, \dots\}$ denote the set of time slots such that the channel state does not change during each time slot. Then, the system state at the n -th time slot is expressed as $\mathbf{q}[n]$. Furthermore, without loss of generality, we scale time and assume that $\lambda + \mu_p + p_a \mu_{mm} + \mu_{\text{sub-6}} = 1$.

We consider the set of control variables $U \triangleq \{(u_0, u_1, u_2, u_3) \mid u_0, u_1, u_2, u_3 \in K\}$. Then, the decision rule at the n -th decision epoch (the beginning of the n -th time slot) is a mapping from the system states to the control variables, i.e., $d_n : Q \rightarrow U$, for all $n \in N$ and the policy π is a sequence of the decision rules, i.e., $\pi = (d_1, d_2, \dots)$. Further, if $\mathbf{q}[n] = \mathbf{q}'$ and $d_n(\mathbf{q}') = (u_0, u_1, u_2, u_3)$ for certain $n \in N$, then if an arrival occurs at the $(n+1)$ -th epoch, we would take actions according to u_0 . Similar explanation applies to u_1, u_2, u_3 . Thus, the transition probabilities in the discrete-time MDP are expressed as

$$\mathbb{P}(\mathbf{q}' \mid \mathbf{q}, \mathbf{u}) = \begin{cases} \lambda & \text{if } \mathbf{q}' = u_0(\mathcal{A}_0(\mathbf{q})) \\ \mu_p & \text{if } \mathbf{q}' = u_1(\mathcal{T}(\mathbf{q})) \\ p_a \mu_{mm} & \text{if } \mathbf{q}' = u_2(\mathcal{D}_1(\mathbf{q})) \\ \mu_{\text{sub-6}} & \text{if } \mathbf{q}' = u_3(\mathcal{D}_2(\mathbf{q})) \end{cases}$$

Then, with the discrete-time MDP, the uniformized problem is formulated as follows:

$$\min_{\pi \in \Pi} \limsup_{N \rightarrow \infty} \frac{1}{N} \mathbb{E}^\pi \left[\sum_{n=1}^N \mathbf{q}[n] \cdot \mathbf{e} \right]. \quad (2)$$

Discounted Delay Problem: To solve the average delay problem, we first consider the problem of minimizing the expected total discounted delay of the system (discounted delay problem) to avoid convergence issues in the presence of bounded value function [21]. Next, we extend our results to the average delay problem. The discounted delay problem in the equivalent discrete-time MDP is expressed as

$$\min_{\pi \in \Pi} \mathbb{E}^\pi \left[\sum_{n=1}^{\infty} \beta^{n-1} \mathbf{q}[n] \cdot \mathbf{e} \right], \quad (3)$$

where β is a discount factor such that $0 \leq \beta < 1$. To solve the discounted delay problem, it is known that there exists an optimal deterministic stationary policy [21]. Thus, we only need to consider the class of deterministic stationary policies. We apply the value iteration method to find the optimal policy.

Under the assumption that the system is stable, value (delay) functions of the initial state $\mathbf{q} \in Q$ are bounded real-valued functions. Let V denote the Banach space of bounded real-valued functions on Q with supremum norm. Define operator $\mathcal{L} : V \rightarrow V$ as

$$\begin{aligned} (\mathcal{L}v)(\mathbf{q}) &\triangleq \mathbf{q} \cdot \mathbf{e} + \beta \min_{\mathbf{u} \in U_{\mathbf{q}}} \left\{ \lambda v(u_0(\mathcal{A}_0(\mathbf{q}))) + \mu_p v(u_1(\mathcal{T}(\mathbf{q}))) \right. \\ &\quad \left. + \mu_{mm} p_a v(u_2(\mathcal{D}_1(\mathbf{q}))) + \mu_{\text{sub-6}} v(u_3(\mathcal{D}_2(\mathbf{q}))) \right\}, \quad (4) \end{aligned}$$

where $v(\cdot) \in V$ and $U_{\mathbf{q}} \subseteq U$ denotes the set of admissible control variables in state \mathbf{q} . Let $J_\beta(\mathbf{q})$ denote optimal expected total discounted delay function of initial state \mathbf{q} . Then, $J_\beta(\mathbf{q})$ is a solution of Bellman function, i.e., $J_\beta(\mathbf{q}) = \mathcal{L}J_\beta(\mathbf{q})$.

III. DELAY OPTIMAL POLICY

A. Discounted Delay Problem

Except that the mmWave channel is extremely intermittent, the average service rate of the mmWave is much higher than

the sub-6 GHz (e.g., two orders of magnitude). Besides, the service rate of the mmWave and processing server are in the same order. Hence, it is reasonable to assume that the expected time for a packet to go through empty mmWave line is less than empty sub-6 GHz interface, i.e., $\frac{1}{p_a \mu_{\text{mm}}} + \frac{1}{\mu_p} < \frac{1}{\mu_{\text{sub-6}}}$. With this assumption, we have the following theorem:

Theorem 1. *Assuming that $\frac{1}{p_a \mu_{\text{mm}}} + \frac{1}{\mu_p} < \frac{1}{\mu_{\text{sub-6}}}$, then we have*

- (a) $J_\beta(A_1(\mathbf{q})) \leq J_\beta(A_h(\mathbf{q}))$ if $q_0 \geq 1, l_1 = 0$;
- (b) $J_\beta(A_2(\mathbf{q})) \leq J_\beta(A_r(\mathbf{q}))$ if $q_0 \geq 1, l_1 + q_1 \geq 1,$
and $l_2 = 0$;
- (c) $J_\beta(\mathcal{T}(\mathbf{q})) \leq J_\beta(\mathbf{q})$ if $l_1 = 1$;
- (d) $J_\beta(A_1(\mathbf{q})) \leq J_\beta(A_2(\mathbf{q}))$ if $\mathbf{q} = (q_0, 0, 0, 0)$
and $q_0 \geq 1$;
- (e) $J_\beta(\mathbf{x}) \leq J_\beta(\mathbf{y})$ if $\|\mathbf{x}\|_1 \leq \|\mathbf{y}\|_1, \mathbf{x}, \mathbf{y} \in Q$.

Proof Idea. Note that zero function (i.e., $v = 0$) satisfies all properties in Theorem 1. Besides, it is known that for any function $v \in V, \lim_{n \rightarrow \infty} \mathcal{L}^{(n)}v = J_\beta$. Thus, in order to show that J_β satisfies all properties in Theorem 1, we start with zero function and show that $\mathcal{L}v$ satisfies the properties if v satisfies the properties in Theorem 1. For the detailed proof, please see our technical report [22]. \square

Note that in the following, if action $A_x \in K$ has a higher priority than action $A_y \in K$, it means that action A_x incurs no more costs than action A_y does, where $x, y \in \{1, 2, r, b, h\}$. Then, from Theorem 1, we obtain the following rules that provides partial characteristics of the optimal policy:

Rule 1. *Holding is not preferable as long as the processing server is idle:* Property (a) implies that action A_1 has priority over action A_h .

Rule 2. *Keeping the mmWave line busy:* Properties (a) and (d) imply that a packet should be scheduled on the mmWave line whenever the mmWave line is empty and the head buffer (see Fig. 4) is not empty.

Rule 3. *Head buffer is the first choice for the sub-6 GHz interface:* By property (b), action A_2 has priority over action A_r . In addition, $J_\beta(\mathcal{T}(\mathbf{q})) = J_\beta(A_{r_p}(\mathbf{q}'))$ and $J_\beta(\mathbf{q}) = J_\beta(A_{r_{\text{mm}}}(\mathbf{q}'))$, where $\mathbf{q} = (q_0, 1, q_1, 1)$ and $\mathbf{q}' = (q_0, 1, q_1 + 1, 0)$. Then, property (c) implies that $A_r(\mathbf{q}') = A_{r_p}(\mathbf{q}')$ for $A_{r_p}, A_{r_{\text{mm}}} \in K_{\mathbf{q}'}$.

Optimal Policy: Based on these rules, we show that optimal policy for the discounted delay problem is of the threshold-type, and is defined as follows:

$$D_m(\mathbf{q}) = \begin{cases} A_1(\mathbf{q}) & \text{if } \mathbf{q} = (q_0, 0, q_1, 1), q_0 \geq 1, \\ & \text{or } \mathbf{q} = (q_0, 0, q_1, 0), q_0 \geq 1, q_0 + q_1 \leq m, \\ A_2(\mathbf{q}) & \text{if } \mathbf{q} = (q_0, 1, q_1, 0), q_0 \geq 1, q_0 + q_1 + 1 > m, \\ & \text{or } \mathbf{q} = (1, 0, q_1, 0), q_1 \geq m, \\ A_r(\mathbf{q}) & \text{if } \mathbf{q} = (0, l_1, q_1, 0), l_1 + q_1 > m, \\ A_b(\mathbf{q}) & \text{if } \mathbf{q} = (q_0, 0, q_1, 0), q_0 + q_1 > m, q_0 \geq 2, \\ A_h(\mathbf{q}) & \text{otherwise,} \end{cases}$$

where D_m is a threshold policy with threshold m such that D_m follows all above rules. Then, for $n \in N$, the decision rule at time slot n is given by $d_n(\mathbf{q}) = (D_m(\mathcal{A}_0(\mathbf{q})), D_m(\mathcal{T}(\mathbf{q})), D_m(\mathcal{D}_1(\mathbf{q})), D_m(\mathcal{D}_2(\mathbf{q})))$.

To prove the optimality of D_m for the discounted delay problem, we name the action sets $\{A_1, A_h\}$ and $\{A_2, A_r\}$ as “not-adding-to-sub-6” and exclusively “adding-to-sub-6”, respectively. We already know the priority between A_1 and A_h and the priority between A_2 and A_r . Thus, it only remains to determine the priority between the sets not-adding-to-sub-6 and adding-to-sub-6. To show this, we dub the path consisting of the head buffer, the processing server, and the mmWave queue as “FastLane”. We claim that in the discounted delay optimal policy, adding-to-sub-6 obtains priority over not-adding-to-sub-6 when the queue length of FastLane exceeds certain threshold m , i.e., a threshold-type policy as expressed by D_m . Next, we show this via value iteration.

Instead of directly utilizing original state space as the variable of value function, we collapse the state space so that state space is reduced from four dimensions to three dimensions. The method of collapsing the state space is similar to that in [16]. However, ours is more involved in that we cannot collapse the state space to two dimensions since we have to capture the event of processing completion. In the case, the system state \mathbf{q} is re-expressed in the form of (x, q_1, l_2) where x denotes the number of packets in the head buffer and processing server. Note that if $x > 0$, then the processing server should be busy by Rule 1. For the sake of exposition in the following proof, we define two terms in Definition 1.

Definition 1. *Let $J_\beta^n(x, q_1, l_2)$ be the optimal expected total discounted delay over the next n time slots with initial state (x, q_1, l_2) . Then, define an intermediate value $T_\beta^n(x, q_1, l_2)$ as*

$$T_\beta^n(x, q_1, l_2) = \begin{cases} J_\beta^n(x, q_1, l_2) & \text{if } \mathbf{q} = \mathbf{0} \text{ or } l_2 = 1 \\ \min\{J_\beta^n(x, q_1, 0), J_\beta^n(x-1, q_1, 1)\} & \text{if } x \geq 1, l_2 = 0 \\ \min\{J_\beta^n(0, q_1, 0), J_\beta^n(0, q_1-1, 1)\} & \text{otherwise} \end{cases}$$

As a result, for $n \geq 0, J_\beta^{n+1}(x, q_1, l_2)$ is written as

$$\begin{aligned} J_\beta^{n+1}(x, q_1, l_2) &= (x + q_1 + l_2) + \beta \lambda T_\beta^n(x + 1, q_1, l_2) \\ &+ \beta \mu_{\text{mm}} p_a T_\beta^n(x, (q_1 - 1)^+, l_2) + \beta \mu_{\text{sub-6}} T_\beta^n(x, q_1, 0) \\ &+ \beta \mu_p T_\beta^n((x - 1)^+, x + q_1 - (x - 1)^+, l_2). \end{aligned} \quad (5)$$

Moreover, $J_\beta^0(x, q_1, l_2) = x + q_1 + l_2$.

Next, we define a class of functions with threshold property, supermodularity and monotonicity in Definition 2 and Lemma 1 proves that J_β^n has these properties.

Definition 2. *Let \mathcal{F} be a class of functions such that for each function $f: \mathbb{N} \times \mathbb{N} \times \{0, 1\} \rightarrow \mathbb{R}_{\geq 0}$ in \mathcal{F} , we have*

$$\begin{aligned} f(x + 1, q_1, 0) + f(x + 1, q_1, 1) \\ \leq f(x, q_1, 1) + f(x + 2, q_1, 0) \end{aligned} \quad (6)$$

$$\begin{aligned} f(x + 1, q_1, 0) + f(x, q_1 + 1, 1) \\ \leq f(x, q_1, 1) + f(x + 1, q_1 + 1, 0) \end{aligned} \quad (7)$$

$$\begin{aligned} f(0, q_1 + 1, 0) + f(0, q_1 + 1, 1) \\ \leq f(0, q_1, 1) + f(0, q_1 + 2, 0) \end{aligned} \quad (8)$$

$$f(x, q_1 + 1, l_2) \leq f(x + 1, q_1, l_2) \quad (9)$$

together with supermodularity:

$$\begin{aligned} f(x, q_1, 1) + f(x + 1, q_1, 0) \\ \leq f(x, q_1, 0) + f(x + 1, q_1, 1) \end{aligned} \quad (10)$$

$$\begin{aligned} f(x, q_1, 1) + f(x, q_1 + 1, 0) \\ \leq f(x, q_1, 0) + f(x, q_1 + 1, 1) \end{aligned} \quad (11)$$

and monotonicity:

$$f(x, q_1, l_2) \leq f(x + 1, q_1, l_2) \quad (12)$$

$$f(x, q_1, l_2) \leq f(x, q_1 + 1, l_2) \quad (13)$$

$$f(x, q_1, 0) \leq f(x, q_1, 1) \quad (14)$$

Eq. (6) to (8) describe the threshold property that is clarified in Lemma 2.

Lemma 1. *The optimal expected total discounted delay over the next n time slots J_β^n satisfies all properties in Definition 2, i.e., $J_\beta^n \in \mathcal{F}$ for each $n \in \mathbb{N}$.*

Proof Idea. Note that $J_\beta^0 \in \mathcal{F}$. By Eq. (5), it remains to show that $T_\beta^n \in \mathcal{F}$ and then $J_\beta^{n+1} \in \mathcal{F}$ given $J_\beta^n \in \mathcal{F}$. For the detailed proof, please see our technical report [22]. \square

Next, we use Lemma 1 to prove that each round of value iteration corresponds to a threshold-type policy as expressed by Lemma 2.

Lemma 2. *For each round of value iteration, the corresponding policy is of the threshold-type.*

Proof Idea. It is known that $J_\beta^n(0, 1, 0) \leq J_\beta^n(1, 0, 0) \leq J_\beta^n(0, 0, 1)$, which means that it's better to hold the packet in FastLane when there is only one packet in the system. Then, we may show that $J_\beta^n(x + 1, q_1, 0) - J_\beta^n(x, q_1, 1)$ or $J_\beta^n(0, q_1 + 1, 0) - J_\beta^n(0, q_1, 1)$ increases as $x + q_1$ increases. In the case, as $x + q_1$ increases, the difference becomes positive, which means that adding-to-sub-6 obtains priority. This can be shown with inequalities and extended inequalities from Lemma 1. For the detailed proof, please see our technical report [22]. \square

Finally, we use Lemma 2 to provide our main result that the optimal policy is of the threshold-type.

Theorem 2. *For the discounted delay optimality problem, there exists an optimal stationary policy that is of the threshold-type with threshold $m \leq \infty$.*

Proof. By Lemma 2, for each round of value iteration, corresponding policy is of threshold-type. Thus, as $n \rightarrow \infty$, the corresponding policy is also of the threshold-type, and the policy is expected total discounted delay optimal policy. \square

Optimal Threshold: Theorem 3 proves that the value of the threshold in the optimal policy of each iteration, increases by at most one unit at the next iteration.

Theorem 3. *If threshold value of the policy corresponding to n -th value iteration is i_n , then the policy corresponding to $n + 1$ -th value iteration has threshold value $i_{n+1} \in [0, i_n + 1]$.*

Proof. We re-express the system state as (y, l_2) , where $y \in \mathbb{N}$ denotes the queue length of FastLane. Then, Lemma 2 is expressed as follows:

$$J_\beta^n(y + 1, 0) < J_\beta^n(y, 1), \text{ if } y \leq i_n - 1; \quad (15)$$

$$J_\beta^n(y + 1, 0) \geq J_\beta^n(y, 1), \text{ if } y \geq i_n. \quad (16)$$

Since $J_\beta^{n+1}(y + 1, 0) - J_\beta^{n+1}(y, 1)$ increases with y , it remains to show that $J_\beta^{n+1}(y + 1, 0) - J_\beta^{n+1}(y, 1) \geq 0$, when $y \geq i_n + 1$. In fact,

$$\begin{aligned} J_\beta^{n+1}(y + 1, 0) - J_\beta^{n+1}(y, 1) \\ = \beta\lambda (T_\beta^n(y + 2, 0) - T_\beta^n(y + 1, 1)) \\ + \beta\mu_p (T_\beta^n(y + 1, 0) - T_\beta^n(y, 1)) + \beta\mu_{\text{mm}} p_a Z \\ + \beta\mu_{\text{sub-6}} (T_\beta^n(y + 1, 0) - T_\beta^n(y, 0)), \end{aligned}$$

where $Z = T_\beta^n(y, 0) - T_\beta^n(y - 1, 1)$ or $Z = T_\beta^n(y + 1, 0) - T_\beta^n(y, 1)$. Note that if $\mathcal{D}_1(y + 1, 0) = (y, 0)$, then $\mathcal{D}_1(y, 1) = (y - 1, 1)$. On the contrary, if we assume that $\mathcal{D}_1(y, 1) = (y, 1)$, then the only packet in the mmWave queue is renege to the sub-6 GHz interface. This only happens when $y = 0$ by the optimal policy, which contradicts with that $y \geq i_n + 1$. Since $y \geq i_n + 1 > i_n$, we have

$$T_\beta^n(y + 1, 0) - T_\beta^n(y, 1) \stackrel{(16)}{=} J_\beta^n(y, 1) - T_\beta^n(y, 1) = 0.$$

Similarly, we obtain that $T_\beta^n(y + 2, 0) - T_\beta^n(y + 1, 1) = 0$ and $T_\beta^n(y, 0) - T_\beta^n(y - 1, 1) = 0$. As for $\mu_{\text{sub-6}}$ term, by monotonicity, we have $T_\beta^n(y + 1, 0) - T_\beta^n(y, 0) \geq 0$. \square

Remark: If we start with policy D_0 and the optimal threshold is m^* , then we can obtain the optimal threshold value in m^* steps via policy iteration.

B. Average Delay Problem

The following theorem extends our results to the average delay problem.

Theorem 4. *There exists an optimal stationary policy of the threshold-type for the average delay problem.*

Proof. According to [23], $\lim_{\beta_n \rightarrow 1} (1 - \beta_n) J_{\beta_n}^{\pi_{\beta_n}^*}(\mathbf{q}) = J^{\pi^*}(\mathbf{q})$, $\forall \mathbf{q} \in \mathcal{Q}$, where $J_{\beta_n}^{\pi_{\beta_n}^*}(\mathbf{q})$ denotes optimal expected total discounted delay under optimal policy $\pi_{\beta_n}^*$ associated with discount factor β_n and $J^{\pi^*}(\mathbf{q})$ denotes optimal average delay under optimal policy π^* . Since our action set is finite, by [23], there exists an optimal stationary policy for the average delay problem such that $\pi_{\beta_n}^* \rightarrow \pi^*$, which implies the optimal policy is of the threshold-type. \square

In order to obtain the optimal threshold for the average delay minimization problem, we note that Theorem 3 also applies to this case as well, and the proof follows the same logic by removing the discount factor β in the proof of Theorem 3.

IV. SIMULATION RESULTS

In this section, we numerically investigate the performance of our proposed policy. To this end, we first investigate the relationship between the arrival rate and the optimal threshold. Next, we demonstrate the benefits of utilizing the sub-6 GHz

paired with our threshold-type policy especially in heavy traffic scenarios. Finally, we compare the performance of our policy against the MaxWeight policy.

A. Relationship between Arrival Rate and Optimal Threshold

We investigate how the arrival rate λ affects the optimal threshold of our policy. In simulations, we set $\mu_{\text{mm}} = \mu_{\text{p}} = 100$, $\mu_{\text{sub-6}} = 1$ and $p_a = 0.6$. Then, we investigate how average delay changes as threshold varies given a value of $\lambda \in \{30, 35, 40, 45, 50, 55\}$. Our simulation results show that for $\lambda = 30, 35, 40$, curves of average delay vs different threshold are similar. For lack of space, we only provide results for $\lambda = 30$ here.

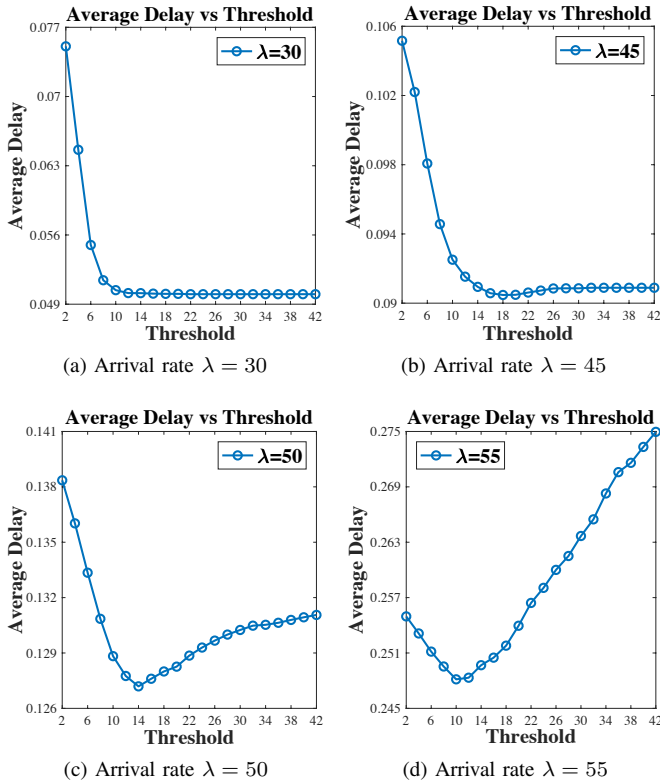


Fig. 5: Average Delay vs Threshold for various arrival rate.

For each result in Fig. 5 (corresponding to a certain λ), the optimal threshold corresponds to the lowest average delay. For example, in Fig. 5b (i.e., $\lambda = 45$), the optimal threshold is 18. As shown in Fig. 5a, we can see that if the arrival rate is not high, a small enough threshold provides low delay and as the threshold increases, the delay does not change much. This is because if packets arrive at system slowly, sum of waiting and service times for each packet in mmWave line will be probably less than service time of the sub-6 GHz server. This implies that the mmWave server does not need the aid of the sub-6 GHz server. On the contrary, adding packets to the sub-6 GHz server increases delay. In addition, Fig. 5b to Fig. 5d demonstrate that the optimal threshold decreases with the arrival rate. This is expected since a faster arrival rate may increase waiting time, which increases the chance of routing through the sub-6 GHz interface.

B. Benefits from the Sub-6 GHz with Threshold-Type Policy

Considering the extremely different service rates of the mmWave and the sub-6 GHz interfaces, would the system delay benefit from the sub-6 GHz interface? In this section, we demonstrate benefits of the sub-6 GHz interface to combat the effects of blockage and intermittent connectivity, especially under heavy traffic scenarios. To this end, we compare delay performance in systems with and without the sub-6 GHz. For the system with the sub-6 GHz (our integrated system), the proposed threshold-type policy is utilized. For the system without the sub-6 GHz server, no scheduling policy applies since only mmWave interface exists in the system. To provide a more clear exhibition of our simulation results, we define relative delay improvement \hat{W} as follows:

$$\hat{W} = \frac{\bar{W}(\text{no sub-6}) - \bar{W}(\text{with sub-6})}{\bar{W}(\text{no sub-6})},$$

where $\bar{W}(\text{with sub-6})$ and $\bar{W}(\text{no sub-6})$ denote the average delay in the integrated system and that in the system without the sub-6 GHz server, respectively.

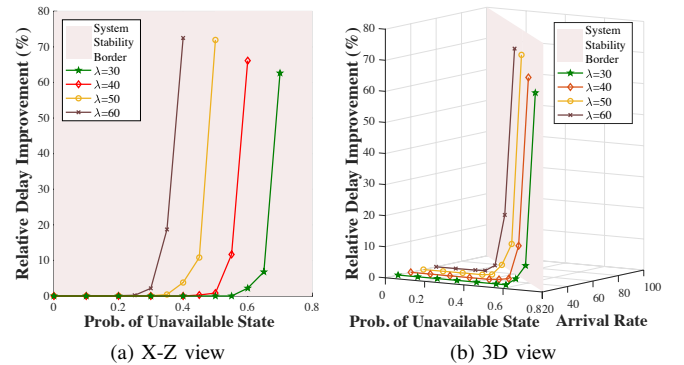


Fig. 6: Delay Performance vs Probability of Unavailable State.

In simulation, we investigate how \hat{W} changes as probability of unavailable state (i.e., p_{na}) increases from 0 to the largest value that ensures stability of the system under fixed arrival rate. We repeat the simulation for different arrival rates. From the results shown in Fig. 6a, we observe that for a certain arrival rate, benefits of the sub-6 GHz interface become more pronounced as the probability of unavailable state increases. For instance, for the arrival rate of $\lambda = 60$, there is up to 70% delay reduction using the integrated architecture paired with the threshold-based policy. Furthermore, in order to exhibit the excellent delay performance in heavy traffic scenarios, in Fig. 6, we introduce a system stability border which is a three dimensional plate that is expressed as $\lambda = \mu_{\text{sub-6}} + (1 - p_{\text{na}})\mu_{\text{mm}}$. As shown in Fig. 6b, the sub-6 GHz interface becomes more beneficial as either the arrival rate or probability of unavailable state increases, i.e., heavy traffic scenarios.

C. Comparison with MaxWeight Policy

In this section, we investigate the performance of the threshold-type policy compared with the MaxWeight policy. Given that the optimal threshold is related to the arrival

rate, for each value of λ , we use the corresponding optimal threshold. From Fig. 7, we note that the threshold-type policy achieves a better delay performance compared with the MaxWeight policy, while it provides a similar throughput performance. We note that the advantage of our threshold-type policy in delay performance over MaxWeight gets smaller when the arrival rate increases.

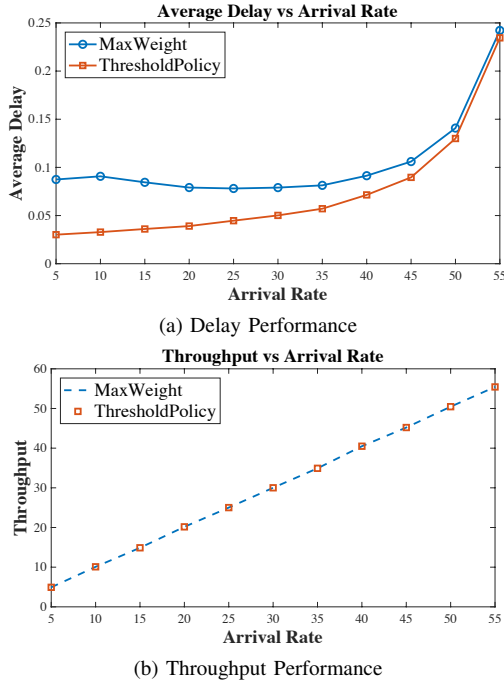


Fig. 7: Delay and throughput performance of our proposed threshold-type policy compared with MaxWeight policy.

V. CONCLUSION

In this paper, we considered an integrated mmWave/sub-6 GHz architecture wherein the sub-6 GHz is used as a fallback mechanism to combat blockage and intermittent nature of the mmWave communication. In this case, packets can be transmitted through the mmWave or sub-6 GHz interface or both. We investigated the optimal scheduling policy such that the expected total discounted delay and the average delay are minimized and showed that the optimal policy is of the threshold-type. Through numerical results, we further demonstrated that utilization of sub-6 GHz paired with our threshold-type policy can highly improve delay performance under heavy traffic, and that the threshold-type policy actually outperforms the MaxWeight policy in delay.

ACKNOWLEDGEMENT

This work has been supported in part by ONR grants N00014-17-1-2417 and N00014-15-1-2166, and National Science Foundation grants CNS-1446582, CNS-1421576, CNS-1518829, CNS-1618566, and CNS-1719371.

REFERENCES

[1] Farooq Khan and Zhouyue Pi. mmWave mobile broadband (MMB): Unleashing the 3–300GHz spectrum. In *34th IEEE Sarnoff Symposium*, 2011.

[2] Theodore S Rappaport, Shu Sun, Rimma Mayzus, Hang Zhao, Yaniv Azar, Kangping Wang, George N Wong, Jocelyn K Schulz, Mathew Samimi, and Felix Gutierrez. Millimeter wave mobile communications for 5G cellular: It will work! *Access, IEEE*, 1:335–349, 2013.

[3] Sanjib Sur, Ioannis Pefkianakis, Xinyu Zhang, and Kyu-Han Kim. Wifi-assisted 60 ghz wireless networks. In *Proceedings of the 23rd Annual International Conference on Mobile Computing and Networking*, pages 28–41. ACM, 2017.

[4] Zulkuf Genc, Umar H Rizvi, Ertan Onur, and Ignas Niemegeers. Robust 60 ghz indoor connectivity: is it possible with reflections? In *Vehicular Technology Conference (VTC 2010-Spring), 2010 IEEE 71st*, pages 1–5. IEEE, 2010.

[5] Christopher Slezak, Vasilii Semkin, Sergey Andreev, Yevgeni Koucheryavy, and Sundeep Rangan. Empirical effects of dynamic human-body blockage in 60 ghz communications. *arXiv preprint arXiv:1811.06139*, 2018.

[6] Sanjib Sur, Vignesh Venkateswaran, Xinyu Zhang, and Parmesh Ramathan. 60 ghz indoor networking through flexible beams: A link-level profiling. In *ACM SIGMETRICS Performance Evaluation Review*, volume 43, pages 71–84. ACM, 2015.

[7] Morteza Hashemi, C Emre Koksal, and Ness B Shroff. Out-of-band millimeter wave beamforming and communications to achieve low latency and high energy efficiency in 5G systems. *IEEE Transactions on Communications*, 66(2):875–888, 2018.

[8] Sumit Singh, Federico Ziliotto, Upamanyu Madhow, Elizabeth M Belding, and Mark JW Rodwell. Millimeter wave wpan: Cross-layer modeling and multi-hop architecture. In *INFOCOM 2007. 26th IEEE International Conference on Computer Communications. IEEE*, pages 2336–2340. IEEE, 2007.

[9] Thomas Nitsche, Adriana B Flores, Edward W Knightly, and Joerg Widmer. Steering with eyes closed: mm-wave beam steering without in-band measurement. In *Computer Communications (INFOCOM), IEEE Conference on*, pages 2416–2424. IEEE, 2015.

[10] Anum Ali, NG Prelcic, and RW Heath. Estimating millimeter wave channels using out-of-band measurements. *Information Theory and Applications Workshop (ITA)*, 2016.

[11] Morteza Hashemi, Ashutosh Sabharwal, C Emre Koksal, and Ness B Shroff. Efficient beam alignment in millimeter wave systems using contextual bandits. In *IEEE INFOCOM 2018-IEEE Conference on Computer Communications*, pages 2393–2401. IEEE, 2018.

[12] Morteza Hashemi, C Emre Koksal, and Ness B Shroff. Energy-efficient power and bandwidth allocation in an integrated sub-6 GHz–millimeter wave system. *arXiv preprint arXiv:1710.00980*, 2017.

[13] Ronald L. Larsen and Ashok K. Agrawala. Control of a heterogeneous two-server exponential queueing system. *IEEE Transactions on Software Engineering*, (4):522–526, 1983.

[14] Woei Lin and P Kumar. Optimal control of a queueing system with two heterogeneous servers. *IEEE Transactions on Automatic control*, 29(8):696–703, 1984.

[15] P WALRAND. A note on optimal control of a queueing system with two heterogeneous serves. *Systems and Control Letters*, 4:131–134, 1984.

[16] Ger Koole. A simple proof of the optimality of a threshold policy in a two-server queueing system. *Systems & Control Letters*, 26(5):301–303, 1995.

[17] VV Rykov. Monotone control of queueing systems with heterogeneous servers. *Queueing systems*, 37(4):391–403, 2001.

[18] Ioannis Viniotis and Anthony Ephremides. Extension of the optimality of the threshold policy in heterogeneous multiserver queueing systems. *IEEE Transactions on Automatic Control*, 33(1):104–109, 1988.

[19] Erhun Özkan and Jeffrey P Kharoufeh. Optimal control of a two-server queueing system with failures. *Probability in the Engineering and Informational Sciences*, 28(4):489–527, 2014.

[20] Leandros Tassioulas and Anthony Ephremides. Stability properties of constrained queueing systems and scheduling policies for maximum throughput in multihop radio networks. *IEEE transactions on automatic control*, 37(12):1936–1948, 1992.

[21] Martin L Puterman. *Markov decision processes: discrete stochastic dynamic programming*. John Wiley & Sons, 2014.

[22] Guidan Yao, Morteza Hashemi, and Ness B Shroff. Integrating sub-6 ghz and millimeter wave to combat blockage: delay-optimal scheduling. *arXiv preprint arXiv:1901.00963*, 2019.

[23] Steven A Lippman. Semi-markov decision processes with unbounded rewards. *Management Science*, 19(7):717–731, 1973.